Eurographics Workshop on Natural Phenomena (2005)
E. Galin, P. Poulin (Editors)

Synthesis of Material Drying History: Phenomenon Modeling, Transferring and Rendering

Jianye Lu, Athinodoros S. Georghiades, Holly Rushmeier, Julie Dorsey and Chen Xu

Department of Computer Science, Yale University, New Haven, CT 06520-8285, U.S.A.

Abstract

We consider the problem of the spatio-temporal variations in material appearance due to the wetting and drying of materials. We conducted a series of experiments that capture the appearance history of surfaces drying. We reduce this history to two parameters that control the shape of a drying curve. We relate these drying parameters to the shape of the original wetted area and the surface geometry. Using these relationships, we generate new time-varying spatial patterns of drying on synthetic shapes.

Categories and Subject Descriptors (according to ACM CCS): I.3.7 [Computer Graphics]: Three-Dimensional Graphics and Realism: Color, shading, shadowing, and texture.

Keywords: Wetting and drying, materials, capture, appearance modeling, realistic rendering.

1. Introduction

Drying is a common natural phenomenon. We notice the effects of drying because wetness alters the appearance of materials—they tend to get darker, and exhibit subtle changes in saturation and hue, when they are wet. We also notice the spatial variations in a material's appearance as it dries. For example, we can judge how long it has been since it rained by whether there are sharp edges between wet and dry regions, or whether the wet areas have started to look soft and splotchy. Figure 1 shows a series of images where we can clearly observe drying, and how far the process has progressed. In this paper, we seek to model the spatio-temporal variations of material appearance caused by drying. In particular, we consider the drying of stone surfaces.

One possible approach to modeling drying is from first principles. First-principles modeling uses conservation of mass, momentum, and energy, and constitutive relationships for basic mechanisms to form equations governing the transfer of fluids within a porous medium. These equations are applied to a model of the material microstructure. Basic principles of optics are used to convert the wholly or partially fluid-filled surface microstructure into a scattering function for the surface. First-principles modeling requires detailed input data for the material being modeled, which is generally not available, and requires considerable computing resources to apply.

Alternatively, appearance-based modeling uses captured data of the drying process to form equations for the time history of the spatial changes of surface reflectance. Two approaches for using the captured data are possible with appearance-based modeling. One approach is to use a pure texture transfer approach, viewing the captured data as a three-dimensional texture. By enforcing continuity in space and time, the history of a wetted area on the captured object can be transferred to a wetted area of a new object. However, such an approach ignores features of the surface geometry, such as concavities and surface orientation, as well as other environmental factors, such as sunlight, which can affect the rate of drying. The alternative is to parameterize the captured results using insights from first-principles modeling to identify appropriate control parameters. In this paper, we adopt this latter appearance-based approach.

We perform experiments to capture the appearance of real surfaces drying. We reduce the drying history at each position on the surface to two parameters that control the shape of the drying curve. These control parameters can vary over the object surface, and we relate these to the object geometry and the shape of the original wetted region. We use these relationships to generate time-varying, spatial patterns of drying on synthetic objects.

2. Background

Wetting and drying phenomenon: It has long been noticed that materials, especially those with rough and absorbent surfaces, look darker when wet. Previous papers in both computer vision and computer graphics have explored this effect. In computer vision, Mall and Lobo [MdVL95]

Figure 1: *Several samples of natural drying. Top row: the top of a stone pillar showing how a drying region fades and diminishes from the boundary inwards; Middle row: a part of a building facade, where concave parts take longer to dry; Bottom row: stone path in a garden, showing a drying pattern that depends not only on the distance from the slate boundaries, but also on the presence of cracks, and possibly on the type of materials and environmental factors, such as wind.*

develop a model for estimating the albedo of a wet surface from a sample of the surface when dry, and vice versa. Their model is adopted from work by Lekner and Dorf [LD88] that demonstrates how total internal reflection at the air/liquid interface results in decreased albedo. They further show that the wet albedo is a non-linear function of dry albedo, with low albedos reduced more by wetting than high albedos. A consequence of this result (not explicitly stated in their paper) is that wet surface color is more saturated than dry surface color, because the wetting further exaggerates the differences in albedo for different wavelengths. We have measured these effects, in particular on stone surfaces. We used a "Digital Swatchbook" spectrophotometer by X-Rite (`http://www.xrite.com/home.aspx`) to measure the reflectance of wet and dry stone. As shown in Figure 2, there is a significant reduction in reflectance across the whole range of the visible spectrum when the surface gets wet. It is also evident that because of this reduction, the dominant surface color becomes more saturated. Figure 9 clearly demonstrates these effects.

In computer graphics, Jensen et al. [JLD99] further refine an optical model for reflection from wet surfaces by combining the models of [LD88] and [TBM86]. In their approach, they account for the effect of the liquid on subsurface scattering within a porous medium and reflections within a thin film of water on the surface using Monte Carlo simulations.

The importance of the spatial variation of material appearance due to wetting was demonstrated by Kass and Miller [KM90]. In computing the flow of water over terrain, they maintain a "wetness" map that indicates whether water has covered an area. The wetness is decreased linearly with time once an area is no longer covered by water. The wetness measure is used to linearly decrease the diffuse reflectance to emulate the darkening of wet material. The results are qualitatively effective, but the rate of drying does not depend on the shape of the wetted area, or the surface geometry.

In [NKON90], Nakamae et al. introduce a more complex model for the spatial variation of reflectance from wet roadway surfaces. In their model, the wetness of a surface is modulated by the water level on a road surface that has shape variations at different scales to account for effects such as the bumpiness of the asphalt and the crown of the roadway. Using water levels, areas are classified as dry, wet, drenched, or puddle. The appearance of dry versus wet areas is modeled by altering the balance of diffuse and specular reflectance. Puddle areas are rendered taking into account the refraction and scattering of light passing through turbid water before reaching the road surface. Drenched surfaces are modeled as a combination of wet and puddle areas. The results are extremely convincing, but specific to the case of roadway surfaces.

In recent work, the effect of water on hair—darkening of its appearance by total internal reflection and added specular reflection—has been modeled in [WGL04]. Though restricted to modeling wet hair, the darkening effect agrees with our observations and measurements of different materials.

Water flow on surfaces: Other papers have dealt with the flow of water on surfaces, such as Dorsey et al.'s work on surface weathering [DPH96, DEJ*99] and Curtis et al.'s work on simulating watercolors [CAS*97]. In these papers, the primary consideration was how the flow of water in a porous medium dispersed other materials, rather than on the appearance of wet materials.

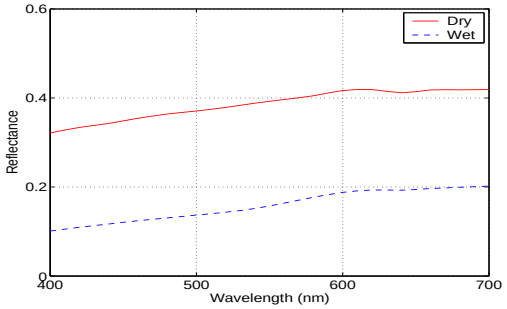

Figure 2: *The reflectance of the stone surface shown in Figure 9 when dry and wet. Note the significant reduction in reflectance across the whole visible spectrum when the surface gets wet, resulting in a more saturated surface color.*

How surfaces get wet in the first place, and how to determine realistic wet region boundaries are important issues. In this paper, we only deal with the appearance history of drying surfaces after they get wet. The work by Chen et al. [CdVLHM97] and Stam [Sta03] simulating flow on surfaces could be used to realistically model the wetting process, including the wet region boundaries.

Weathering effects: Methods for simulating weathering effects have recently become of great interest to researchers because of their potential to reproduce the appearance of imperfect objects. Since the environmental interactions and appearance models involved in simulating the appearance of weathered objects are quite complex, researchers tend to work on special cases of various weathering effects on different materials. Some existing systems model the underlying physical/chemical process, such as metallic patinas [DH96], aging stones [DPH96], and flow and changes in appearance [DEJ*99]. All these systems require thorough understanding of the underlying processes and detailed input data, and often can be computationally demanding.

Hsu et al. maintain a "dust map" to visually simulate the effect of dust accumulation [HW95]. Similar to our paper, their system relates the adjustment of the "dust map" to internal and external factors without simulating the actual environmental process. Yet, their approach is applied on virtual objects with hand-tuned parameter values, which is ad-hoc and can be time-consuming in practice. In contrast, in our work the values of all the parameters come from controlled measurements, and the synthesized images are compared side-by-side with the ground truth.

Material histories: In previous work, we have developed a methodology for defining "material histories" for aging and weathering effects on surfaces [GLX*05]. In that work, examples are given of materials that develop unique, spatio-temporally varying textures as a result of aging. We used parameterized texture transfer, based on a single geometric parameter, to generate unique material histories on synthetic objects. By contrast, in this paper we demonstrate that observed drying effects can be transferred as a deterministic function of the shape of the wetted region and surface geometry, rather than as a texture transfer process with a single control parameter. We consider stone specifically, but believe that our model, using different parameter values, could

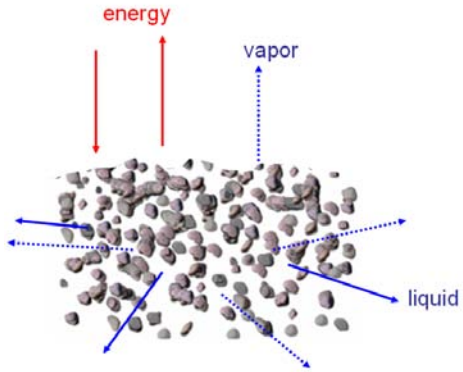

Figure 3: *The drying process for a fluid and a porous material.*

be applied to any porous material. In the next section, we describe the information and experiments we used to construct a model for drying.

3. Modeling the Drying Phenomenon

There are two types of effects we need to capture and model: first, the appearance of the material when it is wet and when it is dry; and second, the process that governs the spatial variation of the wet and dry areas as the material dries. Unlike previous work that attempts to predict wet appearance from dry (or vice versa), e.g. [MdVL95], we simply capture the appearance of the fully dry and fully wet material. By "fully wet," we mean the material has absorbed enough water that no further appearance changes are visible, when there is no puddling or a film of water on the surface.

The more difficult problem is modeling the drying process. We developed our model from a series of experiments on stone surfaces made of fairly homogeneous material. These experiments were designed based on information from the literature on first-principles modeling of drying (e.g. [SW04]). In Figure 3, we show the drying process for a fluid (in our experiments water) and a porous material (in our experiments stone). Energy is transferred to the material either by radiant transport (e.g., exposure to sunlight), or convection from the ambient air. Energy is transferred away from the material as the fluid absorbs energy and is transformed into the vapor state and then advected away by the air. The fluid, in either vapor or liquid form, can move within the material. This movement may be by diffusion, driven by either thermal or density gradients, or it may be due to capillary forces or internal pressure gradients. Gravity also affects the motion, but is a much smaller force within the material.

We make no attempt to explicitly model this transfer, but conclude the following:

- Radiant energy sources and air motion have a major effect on the energy transfer, and so does the evaporation rate. To hold these effects relatively constant, we restrict our experiments to indoor environments. We have no direct sunlight or other intense light introducing strong directional effects on drying. We consider relatively still air, so that the only air motion is the natural convection produced by the drying process itself.

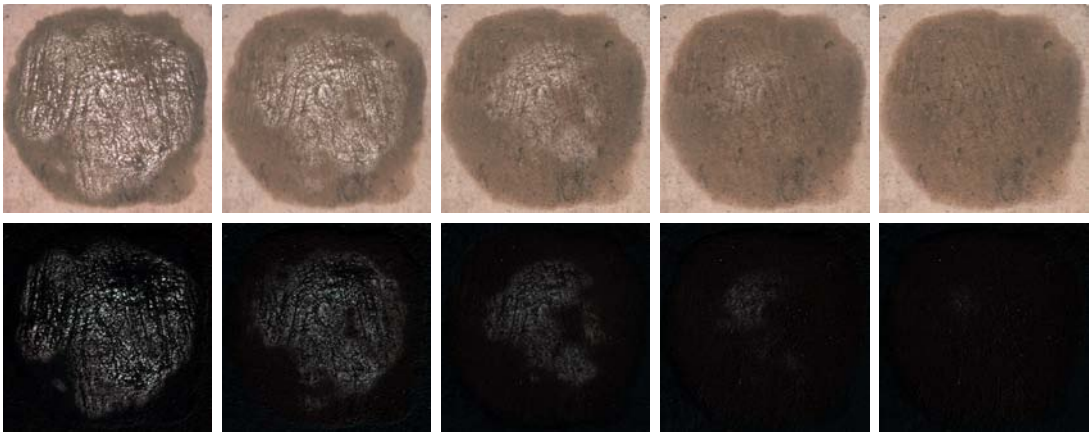

Figure 4: *A sequence of images (top row) of a sample stone right after it was wetted. Its specular component (bottom row) was separated using polarizers at the light source and the camera. (The specular component is in the same scale as the images in the top row, and can be better viewed if zoomed in.)*

- Exposure of the surface to air is an important variable that is not a function of where the process is observed, but on the shape of the surface itself. Our experiments and model must account for the effect of the geometry of the object, restricting the flow of energy and vapor to and from the surface.
- Gradients of the fluid within the porous material are important, so the geometry of the wetted region itself, i.e., the distance of any point on the surface from dry material, is also a significant factor in the drying history of that point.

In our experiments, then, we restrict the environmental variables and observe the variations in drying with the object shape and the shape of the wetted area. In our model, the extent to which the object shape restricts the flow of energy and vapor to and from the surface is quantified by accessibility [Con86, Mil94]. The effect of the shape of the wet region is, as mentioned above, assumed to be a function of the distance of a point on the surface from the boundary of the initial, wet region. These two parameters, which can be readily determined, are assumed to be the main controls of the drying process of a point on the surface, and hence its appearance history.

We model diffuse appearance as a weighted sum of the captured, fully wet and fully dry appearance. The weight, which we call "wetness" and define as in [KM90] to range between 0 and 1, is a measure of how much the process of drying has progressed, and hence how much the appearance has changed from completely wet to completely dry. As mentioned before, the fully wet appearance is determined when there is no puddling or a film of water on the surface. This, in essence, accounts for bulk reflectance effects from subsurface scattering. More often than not, though, a film of water does exist on the surface, especially right after the surface gets wet. This adds a surface (specular) reflectance term to the appearance, which persists for some time as a point on the surface begins to dry.

We used polarizers at the light source and the camera to separate the specular and diffuse components of a wet stone sample. Figure 4 shows a series of images of a stone sample right after it was wetted. The top row shows the original sequence, while the bottom row shows the separated specular component. Note that initially the specularities are significantly brighter than the diffuse component, but more importantly, as the surface water evaporates, or gets absorbed by the material, the specular region shrinks and its intensity decreases as a function of the distance from the wet region boundary. The appearance of the diffuse component, on the other hand, does not change appreciably (except somewhat at the wet/dry interface), signifying little or no drying within the time it took for the specular component to diminish to zero. Our measurements agree with and therefore validate the approach of Nakamae et al. [NKON90], where they model appearance of wet versus dry regions by altering the balance of diffuse and specular reflectance. In Section 4.3, we incorporate a decaying specular component when we synthesize the appearance of spatially varying drying patterns on synthetic objects. For a point on the surface, the magnitude of its specular component is assumed to decay to zero, when its wetness value reaches a threshold.

Although wetness controls the optical appearance through the forward model, in our controlled experiments, where we try to determine the relationship between drying and geometry, we measure wetness through the reverse optical model. (See Section 4.2 for more details.) Wetness is itself a function of the object geometry and the distance to the wet/dry boundary, and hence can vary spatially.

4. Experimental Procedure

We performed preliminary experiments to determine the relationship of wetness to the object geometry and the shape of the initial wetted area. Figure 5 shows experiments isolating the effects of distance to the boundary of the wetted area and of the object shape. We first consider a flat surface, shown in Figure 5a, that isolates the effect of the distance on wetness. This experiment shows the entire wet region drying to some extent, but with points closer to the boundary drying more rapidly. The wetted area shrinks and its boundary

(a) (b)

Figure 5: *Preliminary tests: (a) drying on a flat surface, showing the dependence of the drying pattern on the distance to the boundary of the initial wetted region; (b) drying on an arbitrary, initially all-wet object that depends on accessibility to the environment. Note that convex regions, such as the nose and chin, dry faster than concave parts, such as the eyes and the mouth.*

becomes less sharp as time progresses. We noted a strong effect of distance up to a point, beyond which distance has little impact.

To isolate the effects of object shape, we consider an object with arbitrary shape that has been completely wetted, i.e., it has no sharp wet/dry boundaries. We observe in Figure 5b that the drying is uneven across the surface of the object. We hypothesized that "anisotropic" accessibility (as defined by Connoly in [Con86]), or surface orientation would be the most important factors causing this variation in drying. Plotting the wetness values of different pixels as a function of both accessibility and orientation, we found a significant correlation to accessibility—drying is slower where the surface is concave. We did not find a significant correlation with surface orientation.

4.1. Data Acquisition

As mentioned above, we seek to determine the relationship between the appearance of drying and the geometry of the object and the wet region boundary. Hence, along with the appearance history captured with a digital camera, we also need to acquire the object geometry.

We capture the appearance under controlled lighting using an Olympus C8080WZ color digital camera, while the object geometry is scanned using a laser scanner. (See Figure 6a for our experimental set-up.) The laser scanner used was a ShapeGrabber (`http://www.shapegrabber.com`) with a SG1002 scan head. The camera is calibrated in terms of the coordinate system of the laser scanner, using the method in [RGG*03], allowing us to project the captured color images as textures on the acquired geometry. The lights were mounted on a frame around the scanner and camera, with the lighting kept constant during the capture of a sequence of images. The capture cycle for a single image was approximately 16 seconds, therefore, we can use the image index as a time stamp. Note that because the lighting, camera, and object configuration is constant, the contributing factor to changes in appearance due to drying is the change of reflectance (albedo) of the material as it dries. We make implicit use of this observation in our data analysis described in the next section, where we define wetness.

4.2. Data Analysis

We have no mechanism for measuring the actual wetness of the surface, or the volume fraction of material occupied by water at any time. Since we are only interested in the impact of wetness on appearance, in our work we define "apparent" wetness to be proportional to the measured intensity at any pixel relative to the value observed when the surface is fully wet or fully dry. Note that this is different from how wetness is defined in the applied optics work referenced above. By computing the wetness according to our definition, each image we capture during the drying process allows us to define a wetness map in the same sense as it is defined in [KM90]. (See Figure 6c for a sequence of apparent wetness maps.) The apparent wetness, w, for each point is simply defined as

$$w(I) = \frac{I - I_{wet}}{I_{dry} - I_{wet}}, \tag{1}$$

where I, I_{dry}, and I_{wet} are the intensity values in the current image, in the completely dry image, and in the completely wet image, respectively. (The intensity is determined from the RGB values by eliminating the hue and saturation information while retaining the luminance.) Using apparent wetness is advantageous, as it decouples the drying process from the underlying texture, which is usually fairly stable during the drying process. Furthermore, as long as the lighting is constant during the acquisition, there is no need to know the exact lighting configuration. This decoupling allows us to more easily analyze the relationship of the time-varying spatial patterns of drying to geometry. It also simplifies generating new drying patterns on synthetic shapes.

Using the above definition of wetness, we can determine a plot of each point's wetness history. While the wetness history varies across the object, in general, we can fit the wetness curve with a sigmoid function:

$$w(I(t)) \approx \frac{1}{1 + e^{-\frac{\ln 9 \cdot (t - t_c)}{t_w}}}, \tag{2}$$

where t_c is the time at which the appearance is halfway between wet and dry, and t_w determines the slope of the sigmoid function at t_c. The fitted transition curves pass through 0.1 and 0.9 at $t = t_c - t_w$ and $t = t_c + t_w$, respectively. (See

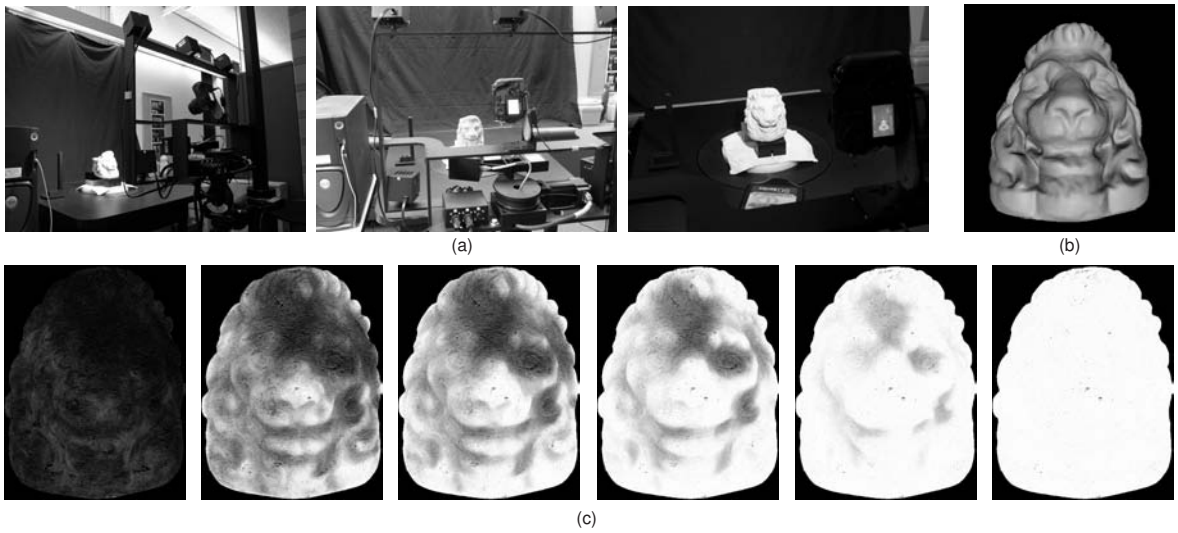

Figure 6: *Data acquisition: (a) the device setup, including the ShapeGrabber scanner, digital camera and turntable; (b) an example of a 3D geometry captured with the ShapeGrabber scanner; (c) a series of wetness maps determined from the captured images of the drying object.*

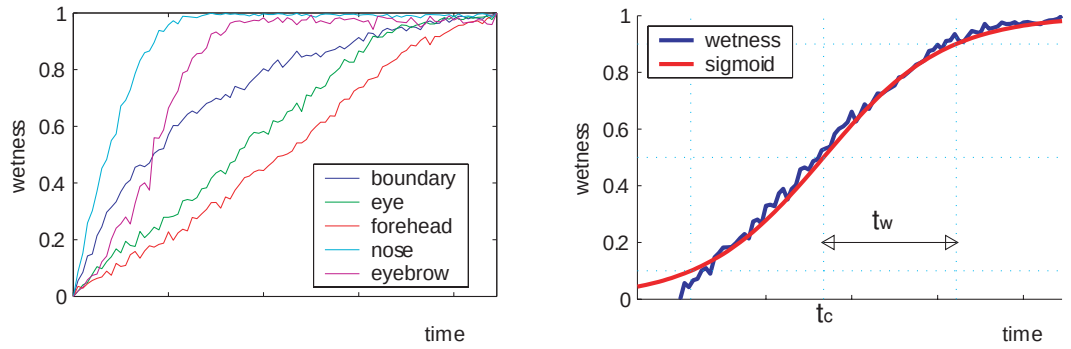

Figure 7: *Wetness transition curves (or drying history) of individual pixels mapping on the 3D object shown in Figures 5b and 6b: (a) Measured wetness transition curves on different parts of the object. Note how curves that lie on convex regions, such as the nose and the eyebrow, transition more quickly, and hence dry faster, while concave regions, such as the eye and the mouth, dry much more slowly. (b) A wetness transition curve fitted with a sigmoid function, where t_c is the time at which the appearance is halfway between wet and dry, and t_w determines the slope of the sigmoid function at t_c. With this fitting, the drying history of a point on the surface is reduced to two parameters.*

Figure 7.) In other words, t_c controls the onset of drying while t_w controls the rate. With this curve fitting, we reduce the wetness history of a pixel to two parameters, greatly simplifying the transfer of wetness patterns to new objects.

Like wetness, t_c and t_w are each functions of accessibility and distance to the original boundary of the wetted region. We assume that this relationship can be approximated by separable functions, and, hence, t_c and t_w can each be separated into two, one-dimensional functions, one of accessibility and one of distance to the boundary. Using the acquired data, we determine these simple, one-dimensional functions, shown in Figures 8a and 8b. For the accessibility plots, we captured image sequences of the initially fully-wet lion statuette, shown in Figures 5b and 6b, while drying. For the distance plots, we used captured images of the drying flat patch, shown in Figure 5a, which lies on the back of the statuette shown in Figure 5b. Note that the functions for t_c and t_w with respect to distance are assumed to be constant beyond 15mm from the wet region boundary—the values beyond 15mm are assumed to be those at 15mm.

We multiply these one-dimensional functions to build 2D lookup maps (shown in Figures 8c and 8d) with respect to both distance and accessibility; one each for t_c and t_w. (Note that before the multiplication, we normalized the functions for t_c and t_w with respect to distance to be from 0 to 1. Hence, they acted as modulation curves on the functions with re-

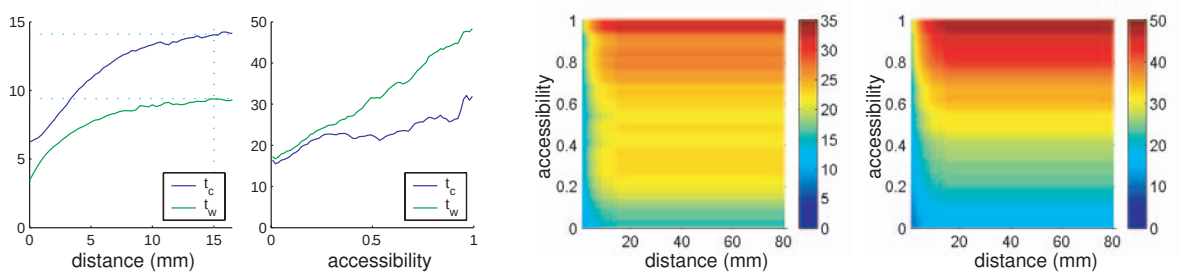

Figure 8: *The lookup maps relating t_c and t_w to accessibility and distance to the boundary of the wetted region: (a) and (b) show the relation of t_c and t_w to distance and accessibility, respectively; (c) the 2D map for t_c; (d) the 2D map for t_w. (The vertical axes in (a) and (b), and the color-bars in (c) and (d) denote time steps. In this case, a time step is equivalent to approximately 16 seconds.)*

spect to accessibility.) We use these 2D maps to deterministically synthesize the spatially varying values of t_c and t_w on new objects. From those values, we can determine the spatially and temporally varying wetness, which is then used to render the appearance history of synthetic drying objects.

4.3. Appearance Transfer and Rendering

Synthesizing the appearance of drying on a new object, consists of two steps. First, the underlying surface texture, in this case stone, is transferred, or synthesized, using standard texture-synthesis techniques [EL99, EF01]. Both the completely wet and the completely dry versions of the texture are synthesized using captured images of the stone when fully wet or fully dry. Figure 9 shows the stone texture we used in synthesizing the underlying texture for the experimental results shown in Figures 11 and 12. The underlying texture contains the high-frequency visual component, which is fairly stable during the drying process.

The drying patterns represented by the wetness maps, which are functions of t_c and t_w (and which themselves are functions of accessibility and distance to the original wet region boundary), affect the low-frequency visual component. Therefore, in the second step of the appearance synthesis, the wetness patterns can, as mentioned above, be transferred deterministically to a new synthetic object.

We find the accessibility and the distance to the wet/dry boundary, and then use the lookup maps, shown in Figure 8, to determine the spatially varying values of t_c and t_w. We then use Equation 2 to determine the wetness maps at each point in time. Using the forward optical model described in Section 3, we determine the synthesized appearance on the synthetic object at different time steps in its drying history. Note that for the diffuse term, the wetness value is used as a weight for interpolating between the fully wet and fully dry appearance. For the specular term, the wetness value is used to determine its decay—it decays to zero when the wetness value reaches 0.1. The specular magnitude is a measure of the proportion of the area projecting to a pixel that is wet, and its decay, and hence the reduction of its relative balance with respect to the diffuse component, is related to the approach of Nakamae et al. [NKON90].

To add the diffuse and specular components together, we need to determine their absolute values. For the diffuse component, we use the Digital Swatchbook spectrophotometer to measure its absolute reflectance, while the specular component is determined from the Fresnel reflectance.

5. Experimental Results

Figure 10 shows two examples of synthetic drying histories on a lion statuette, compared with the ground truth. For the synthetic histories, the shape of the original wetted region was the same as, and extracted from, the ground-truth sequence. In both synthetic examples, we determined the distance of all wet points to the boundary of the original wet regions, as well as the accessibility. We then used the lookup maps shown in Figure 8 to determine the spatially varying values of t_c and t_w. From Equation 2, we determine the time-varying wetness maps for both examples, and then used the forward optical model, described in Section 4.3, to render the appearance history of the drying patches. (Note that no specular component is present in the sequences.) Though the synthetic and the ground-truth drying sequences do not necessarily coincide in time, due to possible inaccuracies in our model, nevertheless, our approach can accurately recreate the *appearance* history of the drying patches. (See the provided movies for the complete drying histories.) This example demonstrates that the combined use of accessibility and distance to the boundary as control parameters can accurately predict the spatial variation of the drying patterns on 3D objects.

Figure 11 shows the synthetic drying history of a partially wet plate with a relief. The original wet region boundary was determined by hand. Like in the previous examples, we used the lookup maps in Figure 8 to determined the spatially varying values for t_c and t_w, which are then used to determine the wetness maps for each time step. The figure shows discrete samples of the drying history of the plate, and demonstrates how our approach can predict the blurring and receding of the wet region boundary, which is the expected result of drying patches. This also demonstrates the realistic decay of the specular component in the synthesized images.

Figure 12 shows the synthesized drying history of a raised mold that was initially fully wet. Note how convex parts of the object, such as the scales, which are more exposed to air convection, dry faster. This figure demonstrates that using

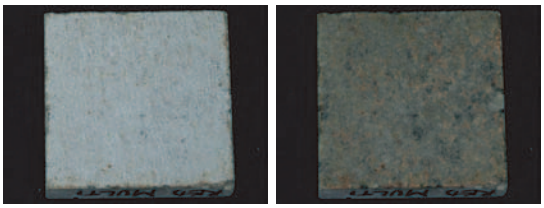

Figure 9: *The dry and wet versions of the stone texture used in synthesizing the underlying texture for the experimental results shown in Figures 11 and 12.*

accessibility as a control parameter can capture the effects of the object geometry on the drying patterns.

6. Conclusions

We have proposed a new synthesis pipeline for determining the appearance history of drying materials. We have also presented a new approach for analyzing the drying phenomenon, greatly simplifying the transfer of wetness patterns from real to synthetic objects. We have demonstrated a scheme for wetness appearance transfer under control parameters, and examined and validated previous optical models for realistic rendering of drying.

Using our definition of wetness, we can reduce the drying history of a point to two parameters. Through a series of experiments that capture the history of drying surfaces, we build lookup maps relating these parameters to the shape of the original wetted region and the surface geometry. It is then a simple matter to transfer these parameters to a new object, creating unique, time-varying wetness maps, which are used to render the synthetic appearance history of the drying object.

While our current model was developed using only stone samples—in still air, and at room temperature—we believe the model would yield plausible results, if applied to other porous media. We may need to change the values of parameters (e.g. overall speed of drying), but the parametric model—with accessibility and distance as the control parameters—would be adequate.

For other types of materials, we could use the same framework, where t_c and t_w are related not only to distance and accessibility, but also to sunlight, air temperature, or air velocity. We provide a baseline model for plausibly adding such other effects.

References

[CAS*97] CURTIS C. J., ANDERSON S. E., SEIMS J. E., FLEISCHER K. W., SALESIN D. H.: Computer-generated watercolor. In *SIGGRAPH '97: Proceedings of the 24th annual conference on Computer graphics and interactive techniques* (1997), ACM Press/Addison-Wesley Publishing Co., pp. 421–430.

[CdVLHM97] CHEN J. X., DA VITORIA LOBO N., HUGHES C. E., MOSHELL J. M.: Real-time fluid simulation in a dynamic virtual environment. *IEEE Computer Graphics Applications 17*, 3 (May 1997), 52–61.

[Con86] CONNOLLY M. L.: Measurement of protein surface shape by solid angles. *J. Mol. Graph. 4*, 1 (1986), 3–6.

[DEJ*99] DORSEY J., EDELMAN A., JENSEN H. W., LEGAKIS J., PEDERSEN H. K.: Modeling and rendering of weathered stone. In *SIGGRAPH '99: Proceedings of the 26th annual conference on Computer graphics and interactive techniques* (New York, NY, USA, 1999), ACM Press/Addison-Wesley Publishing Co., pp. 225–234.

[DH96] DORSEY J., HANRAHAN P.: Modeling and rendering of metallic patinas. In *SIGGRAPH '96: Proceedings of the 23rd annual conference on Computer graphics and interactive techniques* (New York, NY, USA, 1996), ACM Press, pp. 387–396.

[DPH96] DORSEY J., PEDERSEN H. K., HANRAHAN P.: Flow and changes in appearance. In *SIGGRAPH '96: Proceedings of the 23rd annual conference on Computer graphics and interactive techniques* (New York, NY, USA, 1996), ACM Press, pp. 411–420.

[EF01] EFROS A. A., FREEMAN W. T.: Image quilting for texture synthesis and transfer. In *SIGGRAPH '01: Proceedings of the 28th annual conference on Computer graphics and interactive techniques* (2001), ACM Press, pp. 341–346.

[EL99] EFROS A. A., LEUNG T. K.: Texture synthesis by non-parametric sampling. In *ICCV '99: Proceedings of the International Conference on Computer Vision-Volume 2* (1999), IEEE Computer Society, pp. 1033–1038.

[GLX*05] GEORGHIADES A. S., LU J., XU C., DORSEY J., RUSHMEIER H.: *Observing and Transferring Material Histories*. Tech. Rep. YALEU/DCS/TR-1329, Yale Univ., June 2005.

[HW95] HSU S., WONG T.: Simulating dust accumulation. *IEEE Comput. Graph. Appl. 15*, 1 (1995), 18–22.

[JLD99] JENSEN H. W., LEGAKIS J., DORSEY J.: Rendering of wet materials. In *Rendering Techniques '99* (1999), Lischinski D., Larson G. W., (Eds.), Springer-Verlag, pp. 273–282.

[KM90] KASS M., MILLER G.: Rapid, stable fluid dynamics for computer graphics. In *SIGGRAPH '90: Proceedings of the 17th annual conference on Computer graphics and interactive techniques* (1990), ACM Press, pp. 49–57.

[LD88] LEKNER J., DORF M. C.: Why some things are darker when wet. *Applied Optics 27* (Apr. 1988), 1278–1280.

[MdVL95] MALL H. B., DA VITORIA LOBO N.: Determining wet surfaces from dry. In *ICCV '95: Proceedings of the International Conference on Computer Vision* (1995), pp. 963–968.

[Mil94] MILLER G.: Efficient algorithms for local and global accessibility shading. In *SIGGRAPH '94: Proceedings of the 21st annual conference on Computer graphics and interactive techniques* (1994), ACM Press, pp. 319–326.

[NKON90] NAKAMAE E., KANEDA K., OKAMOTO T., NISHITA T.: A lighting model aiming at drive simulators. In *SIGGRAPH '90: Proceedings of the 17th annual conference on Computer graphics and interactive techniques* (New York, NY, USA, 1990), ACM Press, pp. 395–404.

[RGG*03] RUSHMEIER H., GOMES J., GIORDANO F., EL-SHISHINY H., MAGERLEIN K., BERNARDINI F.: Design and use of an in-museum system for artifact capture. In *IEEE/CVPR Workshop on Applications of Computer Vision in Archaeology* (June 2003).

[Sta03] STAM J.: Flows on surfaces of arbitrary topology. *ACM Trans. Graph. 22*, 3 (2003), 724–731.

[SW04] SHI M., WANG X.: Investigation on moisture transfer mechanism in porous media during rapid drying process. *Drying Technology 22*, 1 & 2 (2004), 111–122.

[TBM86] TWOMEY S. A., BOHREN C. F., MERGENTHALER J. L.: Reflectance and albedo differences between wet and dry surfaces. *Applied Optics 25* (Feb. 1986), 431–437.

[WGL04] WARD K., GALOPPO N., LIN M. C.: Modeling hair influenced by water and styling products. In *Proceedings of the 17th International Conference on Computer Animation and Social Agents* (2004), Computer Graphics Society, pp. 207–214.

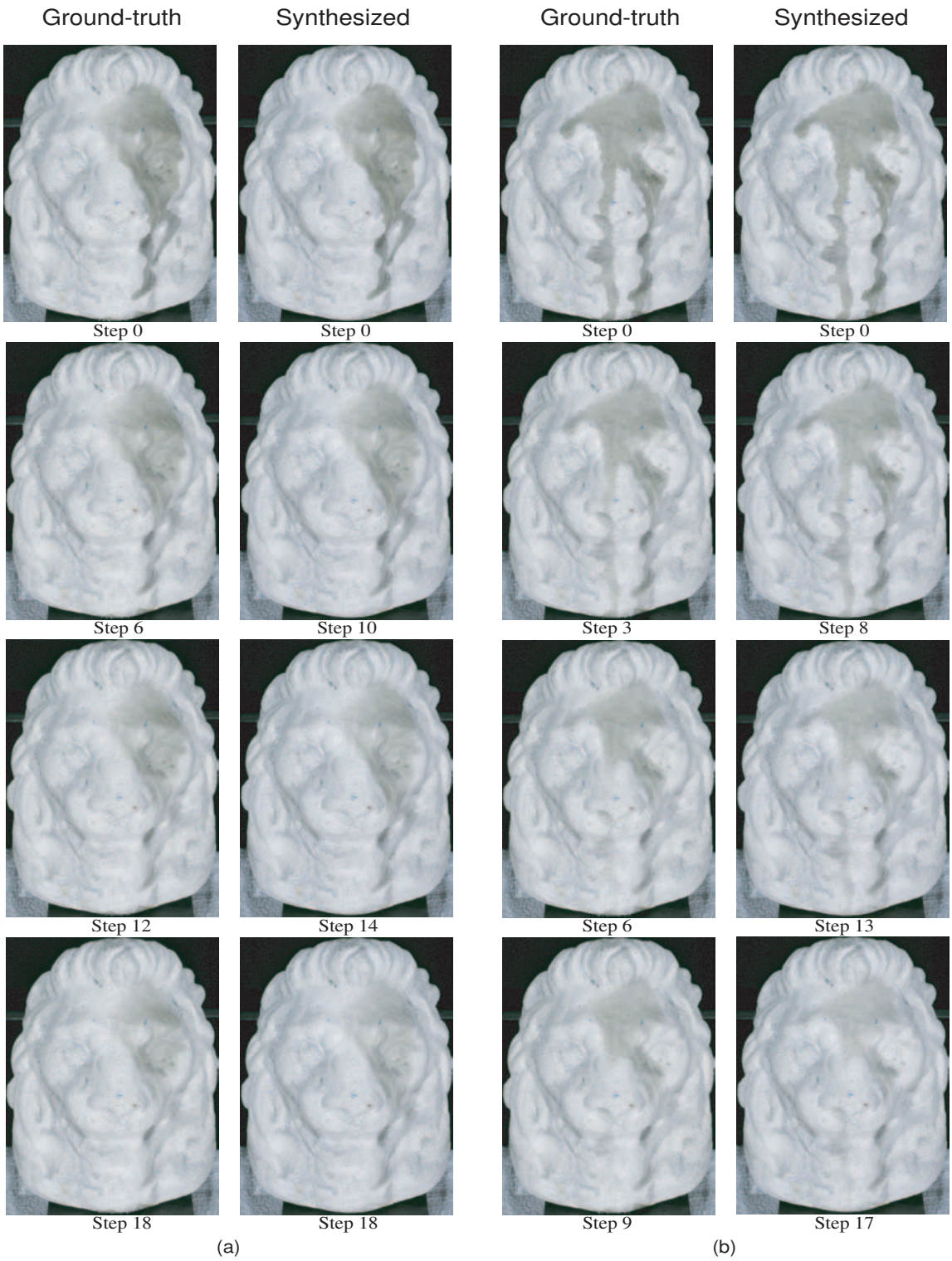

Figure 10: *Two examples of synthetic drying histories on the lion statuette, compared with the ground-truth. The similarities validate the use of the combination of distance and accessibility as control parameters for accurately predicting the spatial variation of drying patterns. (See the movies video/lioncrying1.avi and video/lioncrying2.avi.)*

Figure 11: *Synthetic drying history of a partially wet plate with a relief. The wet region's boundary recedes and becomes blurry as time progresses, which is the expected outcome for drying patches. This example also demonstrates the realistic decay of the specular component.*

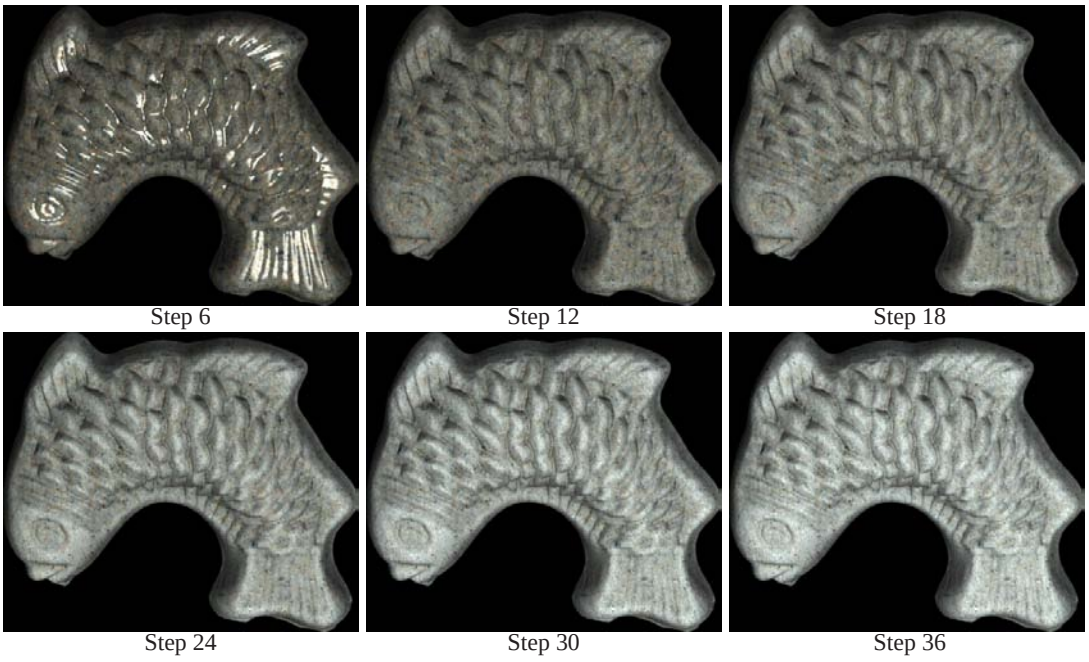

Figure 12: *The synthetic drying history of a raised mold that was initially completely wet. Note how the scales and other convex parts dry faster than concave regions. This demonstrates that using accessibility as a control parameter can capture the effects of the object geometry on the drying patterns. Convex regions are more accessible to natural air convection, and hence dry faster. (See the movie video/fishmold.avi.)*